DESY Summer Student
Programme 2011

First Look at Transverse Polarization Measurement at 250 GeV (ILC/CLIC)

LC Group

Author:
Itai Ben Mordechai
Tel Aviv University

Supervisor:
Dr. Sabine Riemann
Dr. Friedrich Staufenbiel

First Look at Transverse Polarization Measurement at 250 GeV (ILC/CLIC)

Abstract

In the following work, I'm going to show a method for measuring the Transverse Polarization (TPOL) of electron (positron) beams in a linear collider (ILC/CLIC) at high energies (up to 250 GeV) using the Compton differential cross section ($\frac{d\sigma}{d\Omega}$). Unlike the longitudinal polarized electron (positron)Compton cross section that only depends on the energy, the transverse polarized Compton cross section has a dependency on the energy and the angular distribution (ϕ), which makes it harder to measure, especially at high energy, where the effect of the polarization on the cross section is really minor.

1 Introduction

In particle physics we have the Standard Model (SM) which proves itself right in more than one occasion but we also know that it doesn't tell the whole story, because of that many theoretical physicists are coming up with a lot of models that go beyond the SM. The physicists plan experiments to perform precision measurements at highest energies. But let's assume we do find events at the Large Hadron Collider (LHC) or any other experiment that cannot be explained within the SM. We have to identify what is the underlying physics model. To answer this question we need a huge amount of data; for instance, the luminosity[1] goal for the LHC is $10\,\mathrm{fb}^{-1}$ and even $100\,\mathrm{fb}^{-1}$ for the upgrade. But this is not all. In order to distinct between the different models we need the information about the initial state, the center-of-mass energy at which the event happened, and the polarization of the colliding particles. This can be achieved at lepton colliders.

For an e^+e^- accelerator at energies of 250 GeV and higher, a linear accelerator is the only real option, since in circular accelerators particles lose energy by synchrotron radiation. This energy loss follows a m^{-4} dependence, hence for light particles as electrons the compensation of the huge energy loss in circular accelerators becomes inefficient for the required energies.

One can say that if the LHC experiments can give us a picture on what happens beyond the SM, the LC will be the magnifying glass that enables us to look at each pixel.

In this work I used only the ILC setup, since in the ILC design is well developed and a space for Longitudinal Polarimetry is foreseen and the TPOL setup is basically the same (section 4.1). Second because of the different specification of CLIC, the polarimetry will be much more harder then at the ILC, and will require larger space and faster detectors.

2 International Linear Collider (ILC)

The ILC is a linear particle accelerator project. It is planned to have collisions at energies starting from 200 GeV to 500 GeV initially, and could be upgraded to 1000 GeV (1 TeV) later on [1]. The basic ILC configuration design was first declared in 2007, in the Reference Design report (RDR) [1]. The Technical Design Report is planned to be ready end of 2012. This work is managed by the team of the Global Design Effort (GDE) which coordinates nearly 300 laboratories and universities around the world. More than 700 people are working on the accelerator design, and another 900 people on detector development.

[1] Number of particles per unit area per unit time times the opacity of the target

2.1 The Layout

The design of the ILC was chosen to get the physical requirements of energies up to 500 GeV and a peak luminosity of $2 \cdot 10^34\,\mathrm{cm}^{-2}\mathrm{s}^{-1}$. Figure 1 shows a schematic view of the overall layout of the ILC, indicating the location of the major subsystems:

- a polarized electron source based on a photocathode DC gun.
- an undulator-based positron source, driven by the main electron beam (number(2) in Figure 1).
- 5 GeV electron positron damping rings (DR) with a circumference of 6.7 km, housed in a common tunnel. Exiting the damping ring, the bunches are six millimeters long and thinner than a human hair (number(1) in Figure 1).
- Two main linear accelerators, one for electrons and one for positrons, accelerate bunches of particles toward the collision area, operating at an average gradient of 31.5 MV/m, with a pulse length of 1.6 ms (number(3) in Figure 1).
- a 4.5 km long beam delivery system, which brings the two beams into collision with a 14 mrad crossing angle at 500 GeV, at a single interaction point which can be shared by two detectors (number(4) in Figure 1).

The polarimeters for the TPOL/LPOL measurements are located 1.2 km before the interaction point (IP) (number(5) in Figure 1).

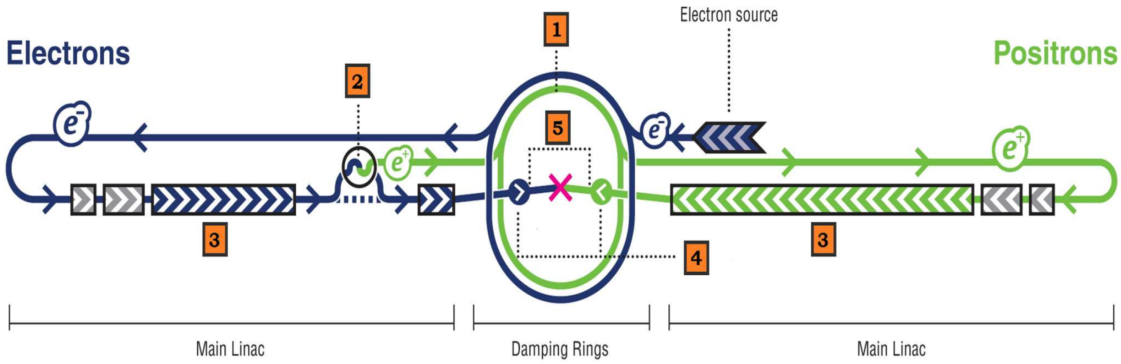

Figure 1: The layout of the ILC [1]

2.2 Beam Parameters

The ILC design has to optimize between accelerator physics and technology challenges. Challenges like beam instability, current, power, background control and many more.
The nominal beam parameter set, corresponding to $E_{cms} = 500GeV$ is given in Table [1].
The nominal IP beam parameters and design ranges are presented in Table [2].

Table 1: Basic design parameters for the ILC

Parameter	Unit	
Center-of-mass energy range	GeV	200 - 500
Peak luminosity	$cm^{-2}s^{-1}$	2×10^34
Average beam current in pulse	mA	9.0
Pulse rate	Hz	5.0
Pulse length (beam)	ms	~ 1
Number of bunches per pulse		1000 - 5400
Charge per bunch	nC	1.6 - 3.2
Accelerating gradient	MV/m	31.5
RF pulse length	ms	1.6
Beam power (per beam)	MW	10.8
Typical beam size at IP	nm	640×5.7
Total AC Power consumption	MW	230
Electrons Polarization		90%
Positrons Polarization		up to 80%

Table 2: Nominal and design range of beam parameters at the IP. The min. and max. columns do not represent consistent sets of parameters, but only indicate the span of the design range for each parameter.

	min	nominal	max	unit
Bunch population	1	2	2	$\times 10^{10}$
Number of bunches	1260	2625	5340	
Linac bunch interval	180	369	500	ns
RMS bunch length	200	300	500	μm
Normalized horizontal emittance at IP	10	10	12	$mm \cdot mrad$
Normalized vertical emittance at IP	0.02	0.047	0.08	$mm \cdot mrad$
Horizontal beta function at IP	10	20	20	mm
Vertical beta function at IP	0.2	0.4	0.6	mm
RMS horizontal beam size at IP	474	640	640	nm
RMS vertical beam size at IP	3.5	5.7	9.9	nm
Vertical disruption parameter	14	19.4	26.1	
Fractional RMS energy loss to beamstrahlung	1.7	2.4	5.5	%

3 Theoretical Background

3.1 Compton Scattering

In 1923, Arthur H. Compton observed the scattering of x-rays from electrons in a carbon target and found scattered x-rays with a longer wavelength than those incident upon the target. The shift of the wavelength increased with the scattering angle according to the Compton formula

$$\lambda_f - \lambda_i = \frac{h}{m_e c}(1 - cos\theta)] \tag{1}$$

where θ is the scattering angle. This discovery is important because it demonstrates that light cannot be explained purely as a wave phenomenon. Compton's work convinced the scientific community that light can behave as a stream of particles (photons) whose energy is proportional to the frequency. This discovery led to his award of the 1927 Nobel Prize in Physics.

Since Compton's discovery in 1923, the Compton scattering process ($e\gamma \rightarrow e\gamma$) was well researched and documented, giving the complete cross section spin dependency [2](in the electron rest frame) :

$$\frac{d\sigma}{d\Omega}(S,P) = \Sigma_0 + S_1(0)\Sigma_1 + S_3[P_Y\Sigma_{2Y} + P_Z\Sigma_{2Z}] \tag{2}$$

$$\Sigma_0 = C[(1 + cos^2(\theta)) + (k_i - k_f)(1 - cos(\theta))] \tag{3}$$

$$\Sigma_1 = C\cos(2\phi)\ sin^2(\theta) \tag{4}$$

$$\Sigma_{2Y} = -Ck_f sin(\phi)sin(\theta)(1 - cos(\theta)) \tag{5}$$

$$\Sigma_{2Z} = -C(1 - cos(\theta))(k_f + ki)cos(\theta) \tag{6}$$

$$k_i = 2\gamma E_\lambda/m_e = 2E_b E_\lambda/m_e^2 \tag{7}$$

$$k_f = 1/(1 - cos(\theta) + 1/k_i) \tag{8}$$

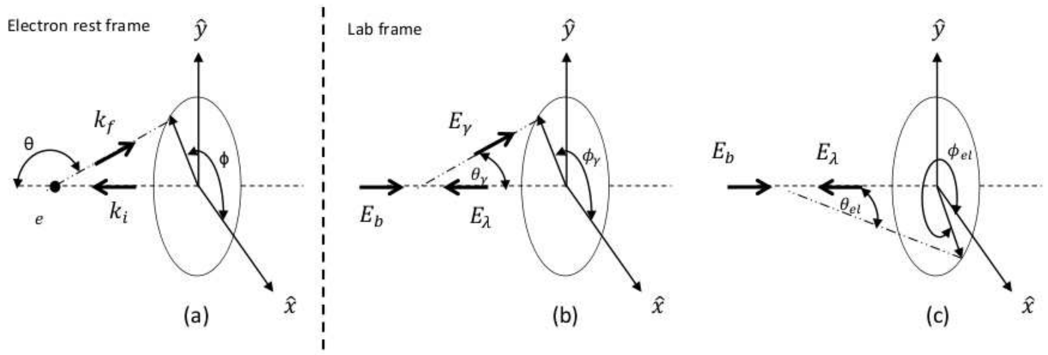

Figure 2: Geometry and coordinate system of Compton scattering,(a) showing the electron rest frame, (b) the laboratory frame with scattering angles of the photon, (c) the laboratory frame with scattering angles of the electron.

$$C = \frac{r_0^2 k_f^2}{2k_i^2} \tag{9}$$

where k_i, k_f donate the momentum of the incoming and the outgoing photon in the electron rest frame, r_0 is the classical electron radius $2.818 \times 10^{-15} m$, S_1, S_3 is the laser longitudinal and transverse helicity[2] (correspondingly), P_Z, P_Y are the electron longitudinal and transverse polarization (correspondingly), E_λ is the laser photon energy and E_b is the electron beam energy.

For our measurement we want to have the cross section in terms of the electron energy in the lab frame, to do that we first make transformation to the photon energy in the lab frame by :

$$cos(\theta) = \frac{E_b - E_\gamma(1 + 1/k_i)}{E_b - E_\gamma} \tag{10}$$

where E_γ is the scattered photon energy in the lab frame. The next step is to go to the scattered electron energy (Figure 2), we do this by using the simple energy conservation law:

$$E_\gamma = E_b + E_\lambda - E_{el} \tag{11}$$

where E_{el} is the energy of the scattered electron in the lab frame.

If we consider that we have full control on the laser helicity, and we set it up to $S_1 = 0$ and if we will look only on electron beam with $P_Z = 0$, we will get the Compton cross section for transverse polarized electrons in terms of the scatter energy $\frac{d\sigma}{dE_{el}^{lab} d\phi}$ (P_Y).

3.2 Magnetic Spectrometer

When a particle passes through a perfect homogeneous magnetic field, it is bent by the Lorentz force in the plane perpendicular to the field direction, with a circular trajectory:

$$R[m] = \frac{P_\perp}{K_b B[T]} \cong \frac{E_{el}[eV]}{K_b B[T]} \tag{12}$$

where the constant $K_b = 0.299792458$ and we use the fact that the particles are relativistic in order to replace the modulus of the momentum by its energy E_{el}[3].

Using equation 12 and some basic geometry one can easily derive the displacement of the particle in the $\hat{x}$ direction, see fig 3(for a particle moving in $\hat{z}$ direction, and magnetic field $B\hat{y}$). And so one can separate between different energies of one relativistic bunch just as a prism separates different colors from white light.

[2] the projection of the spin $\vec{S}$ onto the direction of momentum $\hat{p}$

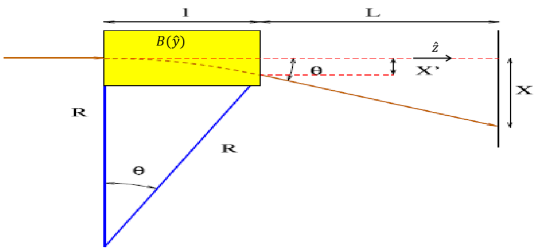

Figure 3: Path of a charged particle inside a magnet with a field perpendicular to the particle momentum.

4 Transverse Polarimetery

Transverse polarization measurement offers a special way to probe for new physics in e^+e^- processes and have been shown to be particularly sensitive to spin-2/graviton exchange for the case of the $e^+e^- \to f\overline{f}\ \ (f \neq e)$ set of final stats. Not only does the TPOL extend the conventional search reach but it also provide a means to uniquely identify spin-2 exchanges [4] or CP violation phenomena (see reference [5]).

4.1 Layout

The TPOL is designed to measure the polarization of an electron (positron) beam with energies up to 250 GeV with an accuracy an accuracy at the per-mils level. Figure 4 shows a schematic view of the overall layout of the TPOL, indicating the location of the major systems:

1. Turning the direction of the beam from its main trajectory .
   - Beam energy: 250 [GeV].
   - Beam horizontal and vertical size : 5 [μm].
2. Compton scattering:
   - Laser Energy: $2.33 \times 10^{-6}[MeV]$ (Green).
   - Crossing angle in radian: 10^{-3}
3. Magnetic spectrometer separates the scattered electrons from the main beam
   - Magnetic field strength: 0.097 [T] as for the 2 first magnets (number(1) in Figure 4).
4. Pixel detector recording the (x,y) position
   - Detector resolution($y \times x$): $10[\mu m] \times 4[mm]$

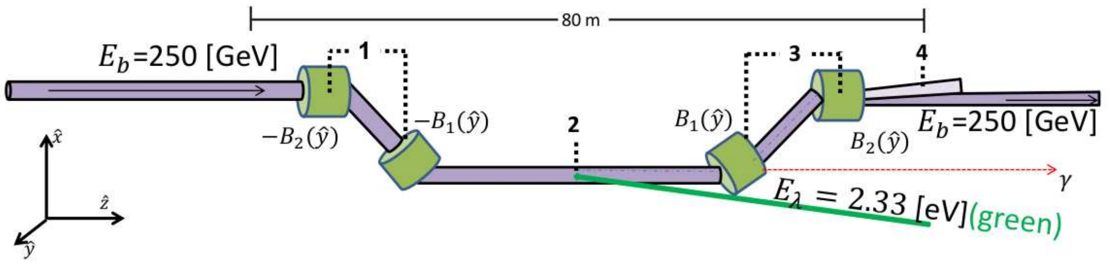

Figure 4: The layout of the TPOL

4.2 The Method

The way to measure the transverse electron polarization is to measure the shift of the mean vertical position ($< y >$) of the scatter electrons distributions when the polarization of the laser light is switched between left and right helicity.

$$y \;=\; D\sin\phi\tan\theta_{el}^{lab} \approx D\sin\phi\,\theta_{el}^{lab} \tag{13}$$

Where D is the distant the electron travels in the $\hat{z}$ direction (after being scattered), and $\theta_{el}^{lab} << 1$.

$$\theta_{el}^{lab} = \frac{Y}{1-Y}\frac{m_e}{E_b}\sqrt{\frac{2k_i}{Y} - (2k_i+1)} \tag{14}$$

$$Y = \frac{E_\gamma}{E_b} = 1 - \frac{E_{el}}{E_b} \tag{15}$$

$$\frac{<y>_L - <y>_R}{2} = P_Y \Pi(E_{el}) \tag{16}$$

where $\Pi(E_{el})$, often referred to as the Analyzing Power (AP), is equal to the shift measured when $P_Y = 1$. In Figure 5 the analyzing power is plotted as a function of the electron energy, with $D = 37.95\,m$.

As we can see from Figure 5, one of the main difficulties in measuring the transverse polarization is the fact that the maximum of the AP is only $\sim 0.035\,mm$, this fact requires a very accurate detector with extreme resolution.

It is important to notice that the $<y>$ dependence on the laser helicity S_3 (L, R) is only in sign, but we will still use both of them. We do this in order to cancel systematic errors and also to compensated for any detector movement (as small as can be) that can occur from the scattered electron transforming momenta to the detector (the L, R helicity will move the detector in opposite directions).

In order to measure the scattered electrons we must separate them from the main beam. We do this by using a magnetic spectrometer, a setup of 4 magnetic fields in $\hat{y}$ direction (see fig 4). The first 2 are used to shift the electron beam parallel to the original direction to a beamline for Compton scattering. The last 2 magnetic fields shift the beam back to its original direction, while the scattered electrons having less energy than original are separated in the $\hat{x}$ direction. The size of this separation is a function of the energy, thus the magnetic field acts on the scattered electrons as a spectrometer (see Fig 6). Using the magnetic spectrometer the energy dependent Compton cross section is translated into an x dependency, and so does the analyzing power $\Pi[E_{el}] \rightarrow \Pi[x]$ (Fig 7).

The transverse polarization P_Y is obtained by two ways: (1) fitting the measured shift $\Delta <y>$ to $P_Y\Pi[x]$ with P_Y as free parameter. (2) As can be seen in Fig 7, the peak

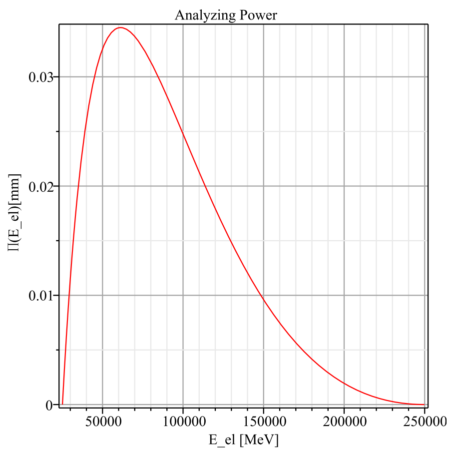

Figure 5: The analyzing power $\Pi(E_{el})$ plotted as a function of the energy of the scattered electrons

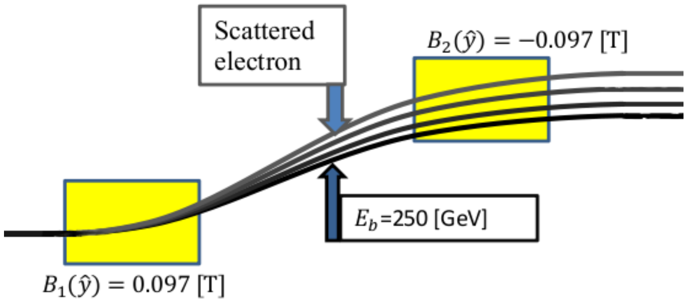

Figure 6: The magnetic spectrometer separated the scattered electrons from the main beam

of the analyzing power is between $40\,mm < x < 100\,mm$ which corresponds to energies between $45\,GeV < E_{El} < 89\,GeV$. To obtain the transverse polarization we will compare the theoretical y asymmetry:

$$A_{theoretical} = \frac{\int_{40}^{100} \Pi(x)\,dx}{60} = 0.0323313 \ \mid \ (D = 37.5m) \tag{17}$$

to the measured one:

$$A_{measured} = \frac{\sum_n y(n)}{\sum_n} \tag{18}$$

where n include all hits in the range. Using eq. 16 we get:

$$\frac{A_{measured}}{A_{theoretical}} = P_Y \tag{19}$$

It is obvious that in the second method we use less data than in the first one, but in a real experiment we will get a lot of noise to our signals and so we are not sure if we will be able to read any data that is not in the specified range.

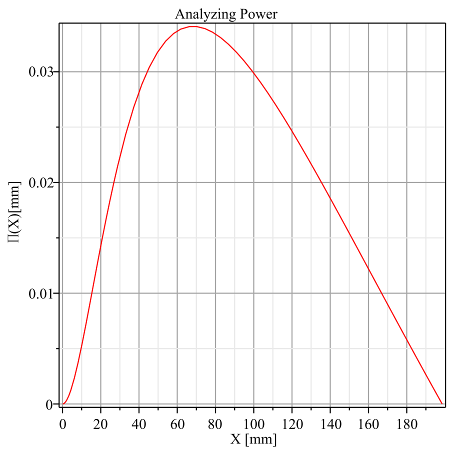

Figure 7: The analyzing power $\Pi(x)$ plotted as a function of the position (x[mm]) of the scattered electrons

5 Monte Carlo Simulation

5.1 The Analyzing Power

Figure 8 shows the measured analyzing power of 100% polarized electron beam, after 1-4 pulses and the fit (P_Y) parameters. As can be seen the first pixle is set at $x = 20\,mm$. Smaller distances correspond to larger electron energies and higher background radiation, so we would need better detector in this area (larger capacity) that withstand the stronger conditions. We can notice that after 3 pulses (7875 bunches, 0.6 sec) we have already started getting great results with less than 0.5% errors. But of course as the polarization goes down we will have to increase the number of pulses we measuring; further, the efficiency of the measurement is less than 100%.

Figure 9 shows the measurement of electrons with 90% polarization and positron 60% polarization (as intended in the ILC). Although the results are good we must consider that in this MC we are able to get the electron (positron) position with resolution of $10\,\mu m$ and we don't have any background noise. That is of course not the real case, but it still

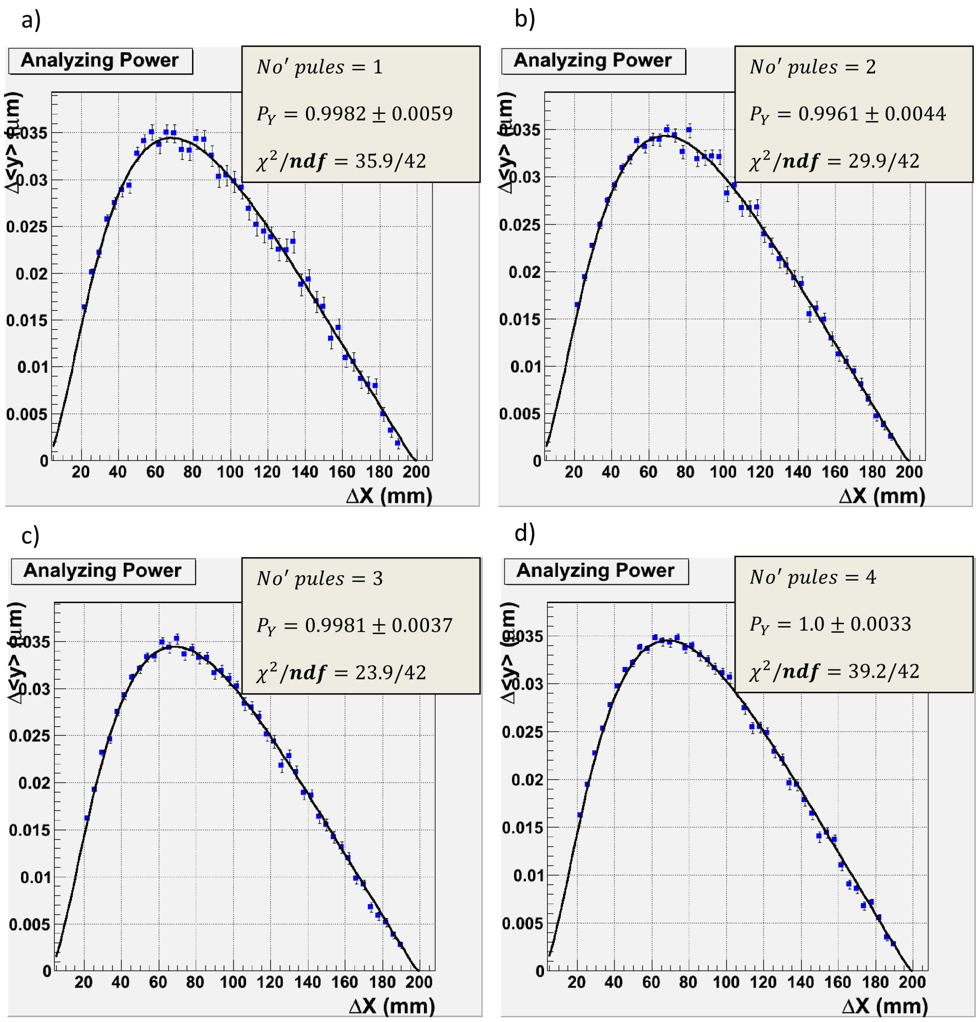

Figure 8: The measured analyzing power for 100% transverse polarized beam fitting to $P_Y\Pi(x)$ (P_Y as free argument), each pulse consist of 2625 bunches

sows as that TPOL with the recruitment errors (less than 0.5%) can be achieved in this method, it becomes a game of the detector resolution, background noise and the geometry of the measurement. A longer distance between spectrometer and detector yields a larger analyzing power to give as a better resolution to our mastermind.

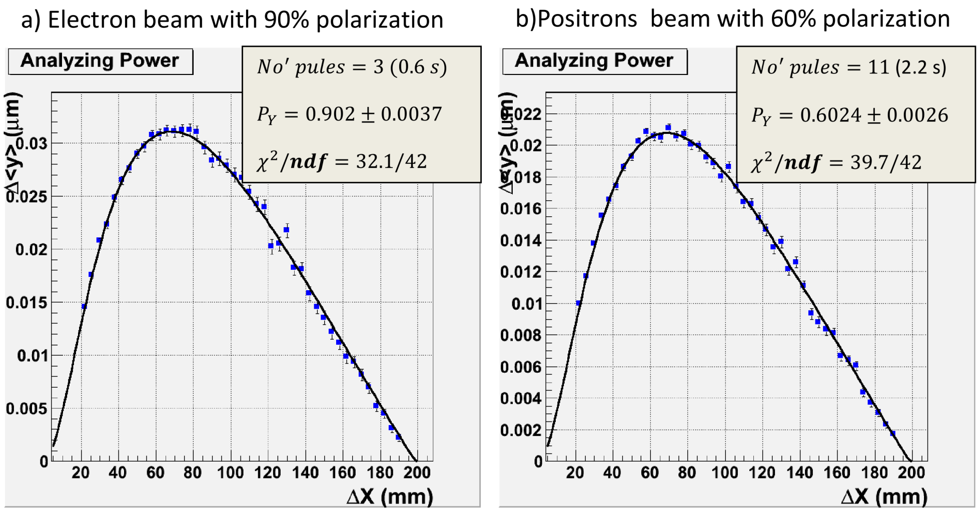

Figure 9: The TPOL measured analyzing power for a) 90% transverse polarization electrons beam. b) 60% transverse polarization positrons beam

5.2 Y Asymmetry

Figure 10 shows the y position of the scattered particles[3], in the x range of $40\,mm < x < 100\,mm$. We can see that even though this method uses less data we also get results which in the required errors. Although this results suffer from the same problem of the previous ones (having no background and $10\,\mu m$ resolution), this method is much less affected by background noise.

6 Conclusion

In this work, I demonstrated a method for TPOL measuring at the ILC, I have shown that by using the Compton scattering process and recording its unique cross section one can calculate the TPOL. We have seen that the problems in measuring the TPOL is not only that it needs full 2D analysis (x and y),but the maximum $< y >$ distance we have with the ILC setup is only 0.35 mm. This fact is the reason for the requirement of $10\,\mu m$ resolution for the detector which could be realized using a pixel detector. Although not much work has been done on the detector, this requirement can be reached with the technology we have today.

In conclusion, although the work is far from being done, from going over all the data we have till now[4], I can say that I do believe that this TPOL measurement method can work in real linear accelerator and not just in the MC simulation.

[3]the left-handed electrons/positrons scattered off the laser beam are entered into the plot with a minus sign

[4]Sap 2011

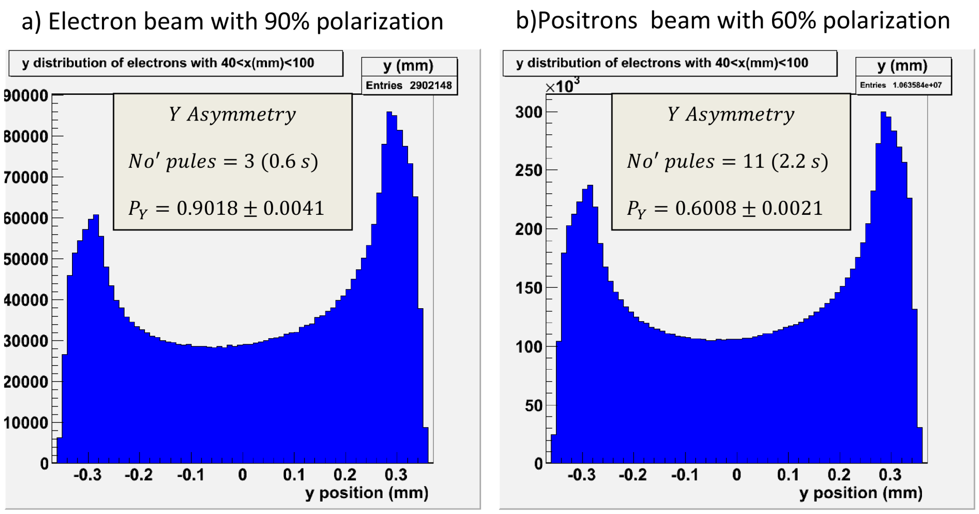

Figure 10: Plots of the scattered electrons (positrons) y position with $40[mm] < x < 100[mm]$ and the TPOL results (using eq.19) a) 90% transverse polarization electrons beam. b) 60% transverse polarization positrons beam

7 Acknowledgement

I will like to thank my instructor in Tel Aviv University Gideon Alexander, my supervisor in DESY Sabine Riemann and Friedrich Staufenbiel, Jenny List from DEST/Hamburg and Karl Jansen, Sabine Baer and all of the DESY / Zeuthen staff for their work on the Summer Student Program 2011. Thank the others, DESY Zeuthen, summer students for the company and help during this time.

References

[1] J. Brau, (Ed.) *et al.* [ILC Collaboration], [arXiv:0712.1950 [physics.acc-ph]].

[2] D. P. Barber, H. D. Bremer, M. Boge, R. Brinkmann, W. Bruckner, C. Buscher, M. Chapman, K. Coulter *et al.*, Nucl. Instrum. Meth. **A329** (1993) 79-111.

[3] M. Viti, ”Precise and Fast Beam Energy Measurement.”, DESY-THESIS-2010-007, February 2010.

[4] T. G. Rizzo,“More transverse polarization signatures of extra dimensions at linear colliders,” JHEP **0308** (2003) 051 [arXiv:hep-ph/0306283].

[5] G. Moortgat-Pick, T. Abe, G. Alexander, B. Ananthanarayan, A. A. Babich, V. Bharadwaj, D. Barber, A. Bartl *et al.*, Phys. Rept. **460** (2008) 131-243. [hep-ph/0507011].

[6] C.Bartels, A.Hartin, C.Helebrant, D.Kfer, J.List: ”Precision Polarimetry at the ILC: Concepts, Simulations and experiments”, arXiv:0909.3960 ,sap 2009.

[7] G. Alexander et al., ”Some aspects of Compton polarimetry for the ILC at the low beam energy around 5-GeV ”, LC-M-2007-014.